DALTON
FULL PAPER

Synthesis and solution studies of ruthenium(II) complexes with thiazole and antileukaemic drug thiopurines. Crystal structure of *trans*-dichlorotris(1,3-thiazole)(triphenylphosphine)ruthenium(II) ‡

Claudia Pifferi and Renzo Cini *,†

Department of Chemical and Biosystem Sciences and Technologies, University of Siena, Pian dei Mantellini 44, I-53100, Siena, Italy

The crystalline complexes $[RuCl_2(PPh_3)_2(thz)_2]$ **1**, $[RuCl_2(PPh_3)(thz)_3]$ **2**, $[Ru(H_2tp)_2(PPh_3)(thz)]Cl_2\cdot 2H_2O$ **3**·$2H_2O$, $[Ru(H_2tg)_2(PPh_3)_2]Cl_2\cdot 2H_2O\cdot EtOH$ **4**·$2H_2O$·EtOH, $[Ru(H_2tprta)_2(PPh_3)_2]Cl_2\cdot 3H_2O$ **5**·$3H_2O$, $[Ru(H_2tp)_2(PPh_3)_2][CF_3SO_3]_2\cdot H_2O\cdot EtOH$ **6**·H_2O·EtOH, $[Ru(H_2tg)_2(PPh_3)_2][CF_3SO_3]_2\cdot 3H_2O$ **7**·$3H_2O$, $[Ru(H_2tp)_2(AsPh_3)(MeOH)]Cl_2\cdot MeOH$ **8**·MeOH, $[Ru(bzim)_2Cl_2(PPh_3)_2]$ **9**, and $[RuCl_2(PPh_3)_2(mpym)_2]$ **10** (H_2tg = purine-2-amino-6-thione, H_2tp = purine-6-thione, H_2tprta = purine-6-thione 2′,3′,5′-tri-*O*-acetylriboside, thz = 1,3-thiazole, bzim = benzimidazole, mpym = 4-methylpyrimidine) have been prepared from $[RuCl_2(PPh_3)_3]$ or $[RuCl_3(AsPh_3)_2(MeOH)]$ and the base in alcoholic solution under nitrogen. The structures of the complexes were investigated by X-ray diffraction (**2**), NMR, conventional spectroscopic techniques and electrochemical methods. All the complex molecules have a pseudo-octahedral co-ordination geometry. The donor set of **2** consists of a phosphorus atom, two chloride anions *trans* to each other and three thz ligands bound to the metal through nitrogen. The sulfur atom of thz does not show any donor ability. However, the thione function of purine is much more active and in complexes **3**–**8** the purine base is chelated through S and N(7) atoms. On refluxing a suspension of **2** and H_2tp in ethanol compound **3** was obtained, which has a slight solubility in water. Electrochemical studies carried out on **7** in acetonitrile revealed a monoelectronic oxidation process at $E_{\frac{1}{2}}$ 1.02 V. The $[Ru^{III}(H_2tg)_2(PPh_3)_2]^{3+}$ species which forms at this potential is relatively stable under the experimental conditions [25 °C; N_2, 1 bar (10^5 Pa)] can be reversibly reduced to the starting compound which was recovered from the mixture. A molecular mechanics analysis, carried out for **1** and **2**, produced a force field for this class of compounds and showed that the *trans*,*trans*,*trans*-$[RuCl_2(PPh_3)_2(thz)_2]$ isomer of **1** is the most stable.

The synthesis and structural characterization of platinum-group metal complexes containing heteroaromatic bases, in particular nucleobases, are important to shed light on the interesting anticancer and antibacterial activity shown by some compounds of Pt^{II}, Ru^{II}, Rh^{II} and Rh^{III}.[1] An interesting approach in the design of metal-based drugs is the preparation of complexes with chemotherapeutic agents as ligands to obtain a sort of synergistic effect.[1a] Attention has recently been devoted to the comprehension of the covalent linkage formation between small molecules containing ruthenium(II) and nucleobases with the aim to simulate the attachment to DNA.[1b,c] A deep structural analysis both in the solid state and in solution of new compounds is often a key step for planning new syntheses as well as to shed light on the conformation of biomolecules. It is well recognized that changes of the oxidation state of metal centres are very important in promoting photochemical and catalytic reactions; therefore, the analysis of redox processes involving metal complexes of biologically or pharmacologically important ligands should often be performed at least in those cases for which the metal ion has two or more easily accessible oxidation states (*e.g.* $Fe^{II,III}$, $Ru^{II,III}$, $Cu^{I,II}$).

6-Thiopurine and its analogues are active against some types of human cancers,[2] and the thiazole system is present in a large number of active drugs.[2d] Furthermore complexes of Ru^{II} and Rh^{III} are valuable probes in investigating nucleic acid structures.[3] For these reasons we have been carrying out investigations on the synthesis of such complexes with thiopurines and thiazole of potential anticancer activity.[4,5] Tertiary phosphine ruthenium complexes are of interest for catalysing a variety of reactions which include homogeneous hydrogenation of alkenes and of imines.[6] Previous studies by us revealed that compounds containing metal-bound phosphines or stibines are promising starting materials to prepare crystalline complexes of the desired purine analogues.[4,5] Here we report on the synthesis and structural characterization of some ruthenium(II) complexes with thiazole and thiopurine derivatives as well as their structural characterization in the solid state [a ruthenium(II)–thiazole derivative] and in solution [all the species, including a ruthenium(II)–nucleoside complex], together with the redox behaviour [for a ruthenium(II)–thioguanine complex]. Finally, a force field suitable for six-co-ordinate ruthenium(II) complexes was set up; it proved to be useful for structural analysis in cases where experimental studies in the solid state or in solution cannot be performed. A density functional analysis was carried out to model some of the ruthenuium(II) complexes.

Experimental

Materials §

The compounds $RuCl_3\cdot 3H_2O$ (Ega), PPh_3 (Erba), $AsPh_3$ (Merck), $Ag(CF_3SO_3)$ (GMBH), H_2tg, H_2tp, Htprta, bzim (Sigma), thz (Janssen) and mpym (Acros) were used without any further purification; $(CD_3)_2SO$ and CD_3OD were 99.5

† E-Mail: cini@unisi.it

‡ *Supplementary data available*: molecular mechanics geometrical parameters, atomic charges, NMR spectra and crystal producing diagram. For direct electronic access http://www.rsc.org/suppdata/dt/1998/2679/, otherwise available from BLDSC (No. SUP 57396, 14 pp.) or the RSC Library. See Instructions for Authors, 1998, Issue 1 (http://www.rsc.org/dalton).

Non-SI unit employed: cal = 4.184 J.

§ H_2tg = purine-2-amino-6-thione; H_2tp = purine-6-thione; H_2tprta = purine-6-thione 2′,3′,5′-tri-*O*-acetylriboside; bzim = benzimidazole; thz = 1,3-thiazole; mpym = 4-methylpyrimidine.

atom% D (Merck) products. Absolute ethyl alcohol, methanol, dichloromethane and acetonitrile analytical grade products were from Merck.

Preparations

Sodium perchlorate was prepared as reported in ref. 7 and $[RuCl_2(PPh_3)_3]$ and $[RuCl_3(AsPh_3)_2(MeOH)]$ were obtained as previously described.[8]

Dichlorobis(thiazole)bis(triphenylphosphine)ruthenium(II), $[RuCl_2(PPh_3)_2(thz)_2]$ 1. Thiazole (0.126 g, 1.48 mmol) and $[RuCl_2(PPh_3)_3]$ (0.297 g, 0.31 mmol) were mixed with absolute ethanol (12 cm^3) previously deoxygenated by flushing dry nitrogen. The brown suspension was refluxed with stirring and under an atmosphere of ultrapure nitrogen for 1 h. After 10 min of reflux an orange solution was obtained. Then a yellow crystalline solid precipitated. The final suspension was cooled to room temperature, the solid collected by suction filtration under nitrogen, and washed with small volumes of cold and deoxygenated EtOH. The product was dried and stored under vacuum at room temperature. Yield 85% (Found: C, 57.85; H, 4.18; Cl, 7.89; N, 3.24; S, 6.90. Calc. for $C_{42}H_{36}Cl_2N_2P_2RuS_2$: C, 58.20; H, 4.19; Cl, 8.18; N, 3.23; S, 7.40%).

Dichlorotris(thiazole)bis(triphenylphosphine)ruthenium(II), $[RuCl_2(PPh_3)(thz)_3]$ 2. Compound **1** (0.245 g, 0.28 mmol) was added to a solution of thz (0.490 g, 5.80 mmol) in ethyl acetate (12 cm^3). The yellow suspension was heated to reflux. Within a few minutes it turned orange. It was refluxed for 2 h and then filtered while hot. The yellow precipitate was washed with ethyl acetate. The crystalline solid was dried under vacuum for 24 h. Yield 60% (Found: C, 47.20; H, 3.52; N, 5.83. Calc. for $C_{27}H_{24}Cl_2N_3PRuS_3$: C, 47.02; H, 3.51; N, 6.09%). Single crystals (red) suitable for X-ray diffraction analysis have been obtained by cooling hot solutions of **1** (5 mg) and thz (14 mg) in ethyl acetate (10 cm^3).

Bis(purine-6-thione)(thiazole)(triphenylphosphine)-ruthenium(II) chloride–water (1/2), $[Ru(H_2tp)_2(PPh_3)(thz)]Cl_2\cdot 2H_2O$ 3·2H_2O. The compound $[RuCl_2(PPh_3)(thz)_3]$ (0.090 g, 0.13 mmol) was added to a clear solution of H_2tp (0.044 g, 0.26 mmol) in absolute ethanol (8 cm^3). The mixture became clear and red after a few minutes of reflux. After *ca.* 2 h of reflux with stirring the hot solution was filtered. The solvent was evaporated in a stream of dry nitrogen at reduced pressure. The red solid was stored under vacuum for 12 h and then mixed with diethyl ether with stirring. The suspension was filtered and the solid dried under vacuum for 2 h. The extraction with ether was repeated two times. Finally the red solid was recrystallized from methanol–ethyl acetate (1 : 7 v/v), filtered and stored under vacuum for 24 h. Yield 25% (Found: C, 42.82; H, 3.01; N, 14.11. Calc. for $C_{31}H_{30}Cl_2N_9O_2PRuS_3$: C, 43.31; H, 3.52; N, 14.66%).

Bis(triphenylphosphine)bis(purine-2-amino-6-thione)-ruthenium(II) chloride–water–ethanol (1/2/1), $[Ru(H_2tg)_2(PPh_3)_2]Cl_2\cdot 2H_2O\cdot EtOH$ 4·2H_2O·EtOH. Purine-2-amino-6-thione (0.34 g, 2 mmol) was mixed with ethanol (20 cm^3). The mixture was deoxygenated by fluxing dry N_2 for half an hour and $[RuCl_2(PPh_3)_3]$ (0.98 g, 1.02 mmol) added. The suspension was refluxed for 3 h with stirring in an atmosphere of dry N_2. On heating, the solid dissolved and the mixture turned gold-yellow. On cooling to room temperature the solution produced a crystalline precipitate. The solid was filtered off and washed twice with EtOH. The crude product was recrystallized twice from EtOH, collected and dried under vacuum. It was stored under vacuum, over silica gel. The solid is stable in the air at room temperature for years. Some efflorescence of the co-crystallized EtOH and H_2O molecules can occur so that the formula depends on the storage conditions. Yield *ca.* 60% (Found: C, 51.20; H, 3.90; N, 12.76; S, 6.3. Calc. for $C_{48}H_{50}Cl_2N_{10}O_3P_2RuS_2$: C, 51.80; H, 4.17; N, 12.59; S, 5.76%).

Bis(purine-6-thione 2′,3′,5′-tri-*O*-acetylriboside)bis(triphenylphosphine)ruthenium(II) chloride–water (1/3), $[Ru(H_2tprta)_2(PPh_3)_2]Cl_2\cdot 3H_2O$, 5·3$H_2O$. The preparation was carried out through a procedure similar to that used for **4**, in ethanol (20 cm^3), under nitrogen, by using $[RuCl_2(PPh_3)_3]$ (0.98 g, 1.02 mmol) and Htprta (0.82 g, 2.00 mmol). The solid consists of yellow small crystals. Yield *ca.* 50% (Found: C, 51.12; H, 4.57; N, 6.88. Calc. for $C_{68}H_{72}Cl_2N_8O_{17}P_2RuS_2$: C, 51.97; H, 4.62; N, 7.13%).

Bis(purine-6-thione)bis(triphenylphosphine)ruthenium(II) trifluoromethanesulfonate–water–ethanol (1/1/1), $[Ru(H_2tp)_2(PPh_3)_2][CF_3SO_3]_2\cdot H_2O\cdot EtOH$ 6·H_2O·EtOH. The compound $[Ru(H_2tp)_2(PPh_3)_2]Cl_2\cdot 2H_2O\cdot 2EtOH$[4b] (1.130 g, 1.00 mmol) was dissolved in EtOH (30 cm^3). The salt $Ag(CF_3SO_3)$ (0.514 g, 2.00 mmol) as a finely ground powder was added. The mixture was stirred in the dark at room temperature for 12 h, then filtered and taken to dryness. The solid was recrystallized from ethanol–diethyl ether. Yield *ca.* 40% (Found: C, 46.32; H, 3.57; N, 8.75. Calc. for $C_{50}H_{46}F_6N_8O_8RuS_4$: C, 46.47; H, 3.59; N, 8.67%).

Bis(purine-2-amino-6-thione)bis(triphenylphosphine)-ruthenium(II) trifluoromethanesulfonate–water (1/3), $[Ru(H_2tg)_2(PPh_3)_2][CF_3SO_3]_2\cdot 3H_2O$ 7·3H_2O. The compound was prepared from **4** (1.113 g, 1.00 mmol) and $Ag(CF_3SO_3)$ (0.514 g, 2.00 mmol) in ethanol (30 cm^3) by a procedure similar to that used for **6**. Yield *ca.* 45% (Found: C, 43.83; H, 3.56; N, 10.34. Calc. for $C_{48}H_{45}F_6N_9O_9P_2RuS_4$: C, 43.92; H, 3.53; N, 10.67%).

(Methanol)bis(purine-6-thione)(triphenylarsine)ruthenium(II) chloride–methanol (1/1), $[Ru(H_2tp)_2(AsPh_3)(MeOH)]Cl_2\cdot$MeOH 8·MeOH. The compound $[RuCl_3(AsPh_3)_2(MeOH)]$ (0.620 g, 0.73 mmol) and $H_2tp\cdot H_2O$ (0.340, 2.00 mmol) were mixed with methanol (20 cm^3). The mixture was refluxed for 3 h then filtered while hot. Diethyl ether (80 cm^3) was added to the orange solution. The orange precipitate formed was filtered off, washed with diethyl ether and then dried under vacuum. The crude product was recrystallized twice from methanol–diethyl ether. Yield *ca.* 50% (Found: C, 42.56; H, 3.69; Cl, 8.37; N, 13.23; S, 7.57. Calc. for $C_{30}H_{31}AsCl_2N_8O_2RuS_2$ C, 43.20; H, 3.63; Cl, 8.08; N, 12.91; S, 7.44%).

Bis(benzimidazole)dichlorobis(triphenylphosphine)ruthenium(II), $[Ru(bzim)_2Cl_2(PPh_3)_2]$ 9. The compound $[RuCl_2(PPh_3)_3]$ (0.098 g, 0.10 mmol) was added to a deoxygenated solution of bzim (0.048 g, 0.41 mmol) in absolute ethanol (6 cm^3). After 5 min of reflux with stirring the brown suspension turned to a clear red solution which produced an orange crystalline solid. The suspension was refluxed for 1 h, then cooled to room temperature and finally filtered under nitrogen. The solid was rinsed with small portions of cold ethanol, dried and stored under vacuum. Yield 65% (Found: C, 64.62; H, 4.74; N, 5.73; P, 6.60. Calc. for $C_{50}H_{42}Cl_2N_4P_2Ru$: C, 64.38; H, 4.54; N, 6.01; P, 6.64%).

Dichlorobis(4-methylpyrimidine)bis(triphenylphosphine)-ruthenium(II), $[RuCl_2(PPh_3)_2(mpym)_2]$ 10. 4-Methylpyrimidine (0.049 g, 0.52 mmol) and $[RuCl_2(PPh_3)_3]$ (0.098 g, 0.10 mmol) were added to absolute ethanol (10 cm^3) previously deoxygenated. The mixture was refluxed under nitrogen. After a few minutes of heating the brown suspension changed to orange. The reflux was maintained for 2 h; then the mixture was cooled to room temperature and filtered. The solid collected was rinsed with EtOH and stored under vacuum for 24 h. Yield 75% (Found: C, 62.12; H, 4.83; N, 6.97. Calc. for $C_{46}H_{42}Cl_2N_4P_2Ru$: C, 62.44; H, 4.78; N, 6.33%).

Spectroscopy

The ^{1}H NMR spectra were recorded in $(CD_3)_2SO$ or $CDCl_3$ solutions at 25 ± 0.1 °C on Varian XL-200 and Brüker AC-200 spectrometers operating at 200 MHz. Tetramethylsilane was the internal reference. The ^{31}P NMR spectra were measured at 25 ± 0.1 °C on a IBM WP-200 SY spectrometer at 81.01 MHz: 5 mm NMR tubes were used for all the samples. Trimethyl phosphate (tmp) was the internal reference. The infrared spectra, as Nujol mulls between CsI plates, or KBr and CsI pellets, were measured on a Perkin-Elmer model 597 or model 1600 spectrometer.

Electrochemistry

Voltammetry. The voltammetric measurements were carried out with a PAR model 170 electrochemistry system; the recording devices were an Amel model 862/A X-Y recorder and a Hewlett-Packard 1123 A storage oscilloscope. The working electrode was a platinum sphere. It was surrounded by a platinum-spiral counter electrode and its potential was measured using a Luggin capillary from the reference electrode compartment.

Coulometry. For the controlled-potential electrolyses an Amel model 551 potentiostat with an associated coulometer model 558 integrator was used. The experiments were carried out by using a H-shaped cell with anodic and cathodic compartments separated by a sintered glass disc. A platinum gauze or a mercury pool was used as working electrode; the counter electrode was a mercury pool.

In all the electroanalytical tests an aqueous saturated calomel electrode (SCE) was used as reference electrode. However the $E_{\frac{1}{2}}$ values are referred to that of the ferrocenium–ferrocene couple, obtained from voltammetric measurements performed in the same solution, in order to eliminate the effect of variable diffusion potentials at the aqueous–non-aqueous interface. The experiments were carried out at 25 ± 0.1 °C.

Crystallography

Powder diffraction. X-Ray powder diffraction data were registered with Cu-Kα radiation, on a Difflex-R OET generator. The powder samples were enclosed in 0.3 mm Lindemann capillaries. The Debye camera had a diameter of 57.3 mm.

Single crystal diffraction. *Data collection.* A red prism of compound **2**, dimensions 0.40 × 0.50 × 0.60 mm, was selected and mounted on a glass fiber for data collection on a Siemens P4 four-circle automatic diffractometer (see Table 1 for details). Preliminary studies for the determination of the space group were carried out through oscillation and Weissenberg techniques. Accurate cell constants were measured on the basis of the values for the angles of 28 randomly selected reflections in the range $10 < 2\theta < 45°$ analysed *via* full-matrix least squares. The data, collected at 293 K, by using Mo-Kα graphite-monochromated radiation (λ 0.710 73 Å), were corrected for Lorentz-polarization and absorption effects (ψ-scan technique based on the reflections 0,−1,−1; −2,0,−6; 2,0,6).

Structure solution and refinement. The structure solution and refinement (based on F^2, mean $|E^2 - 1|$ 0.903; 0.968 for centrosymmetric and 0.736 for non-centrosymmetric space group; trials to solve the structure of the space group $P1$ were not successful as all the non-hydrogen atoms of the asymmetric unit could not be located) was carried out through the automatic Patterson and full-matrix least-squares methods of SHELXS 86.[9]

The Fourier-difference analysis showed peaks of relatively high intensity around the atoms C(41) and S(1) of one of the thz ligands. This was interpreted as a statistical disorder of the thz(1) molecule around a non-crystallographic twofold axis along the N[thz(1)]–Ru bond. The coordinates of the two new peaks were assigned as atoms C(41B) and S(1B) and included in the refinement. The site occupancy factors (SOFs) of the C(41), C(41B), S(1) and S(1B) atoms were constrained as follows: SOF[C(41)] = SOF[S(1)]; SOF[C(41B)] = SOF[S(1B)] and SOF[C(41)] + SOF[S(1B)] = 1. The C(21)–S(1), C(41)–S(1), C(41B)–S(1B) and C(51)–S(1B) bond distances were constrained to 1.70 ± 0.02 Å whereas the C(41)–C(51), C(21)–C(41B) bond lengths were fixed at 1.36 ± 0.02 Å. A similar disorder was not found for the ligand molecules thz(2) and thz(3). All the H atoms were set in calculated position *via* the HFIX instruction of SHELXL 93[10] and their thermal parameters were constrained to be 1.2 times U_{eq} of the atoms to which they are bound. The refinement converged to $R1 = 0.0556$ and $wR2 = 0.1403$ over 3971 reflections with $I > 2\sigma(I)$. The scattering factors were those of SHELXS 86 and SHELXL 93. All the calculations were carried out on VAX 6610 and OLIDATA Pentium 75 Hz machines using SHELXS and PARST[11] packages.

CCDC reference number 186/1030.

See http://www.rsc.org/suppdata/dt/1998/2679/ for crystallographic files in .cif format.

Table 1 Selected crystal data and structure refinement for $[RuCl_2(PPh_3)(thz)_3]$ **2**

Empirical formula	$C_{27}H_{24}Cl_2N_3PRuS_3$
M	689.61
Space group	$P\bar{1}$ (no. 2)
Crystal system	Triclinic
a/Å	9.355(3)
b/Å	11.152(3)
c/Å	14.225(4)
α/°	88.55(2)
β/°	76.89(2)
γ/°	80.32(2)
U/Å^3	1424.7(7)
Z	2
D_c/Mg m^{-3}	1.608
μ/mm^{-1}	1.037
$F(000)$	696
Data, restraints, parameters	3971, 9, 362
Final $R1$, $wR2$ [$I > 2\sigma(I)$]	0.0556, 0.1403
(all data)	0.0765, 0.1640

Molecular mechanics and density functional analysis

Molecular mechanics calculations have been carried out through the MACROMODEL 5.0 package[12] implemented on a Indigo 2-Silicon Graphics work station. The total strain energy was computed as the sum: $E_{tot} = E_b + E_\theta + E_\varphi + E_{nb} + E_{hb} + E_\varepsilon + E_{solv}$ (bond-length deformation, valence-angle deformation, torsion angle deformation, non-bonding interaction, hydrogen-bonding interaction, electrostatic interaction and solvation contribution). The force field is essentially AMBER[13] implemented in MACROMODEL 5.0. Modification and extension of the force field was obtained *via* a trial-and-error procedure which gave excellent agreement between calculated and observed structures. Starting values were obtained by applying Badger's rule,[14,15] using the parameters by Herschbach and Laurie[16] (stretching) and Halgren's equation[17,18] (bending). The initial values for the parameters of the latter equations were based on those reported in ref. 19 for some ruthenium–sulfoxide compounds.

The new force field parameters are reported in Table 4. The total strain energy, E_{tot}, was minimized through the Polak–Ribiere conjugate gradient minimization method until the root mean square (r.m.s.) value of the first derivative vector was less than 0.01 kJ mol^{-1} Å^{-1}. The starting structure was that found for the solid state *via* single crystal X-ray diffraction. The atomic charges used to compute the electrostatic and solvation

Table 2 Selected bond lengths (Å) and angles (°) for [$RuCl_2(PPh_3)(thz)_3$] **2**

Ru–N(1)	2.082(5)	S(2)–C(22)	1.685(6)
Ru–N(2)	2.106(5)	S(3)–C(43)	1.689(8)
Ru–N(3)	2.183(5)	S(3)–C(23)	1.699(7)
Ru–P	2.299(2)	N(1)–C(21)	1.341(8)
Ru–Cl(1)	2.409(2)	N(1)–C(51)	1.359(8)
Ru–Cl(2)	2.425(2)	N(2)–C(22)	1.322(9)
P–C(1C)	1.839(6)	N(2)–C(52)	1.375(9)
P–C(1B)	1.838(6)	N(3)–C(23)	1.276(9)
P–C(1A)	1.858(6)	N(3)–C(53)	1.381(8)
S(1)–C(21)	1.693(7)	C(41)–C(51)	1.35(2)
S(1)–C(41)	1.71(2)	C(42)–C(52)	1.418(7)
S(2)–C(42)	1.659(6)	C(43)–C(53)	1.394(10)
N(1)–Ru–N(2)	173.2(2)	C(21)–N(1)–C(51)	109.7(5)
N(1)–Ru–N(3)	83.4(2)	C(21)–N(1)–Ru	126.1(4)
N(2)–Ru–N(3)	90.3(2)	C(51)–N(1)–Ru	123.9(4)
N(1)–Ru–P	92.13(14)	C(22)–N(2)–C(52)	109.1(6)
N(2)–Ru–P	94.3(2)	C(22)–N(2)–Ru	125.6(5)
N(3)–Ru–P	174.46(14)	C(52)–N(2)–Ru	125.3(4)
N(1)–Ru–Cl(1)	93.00(14)	C(23)–N(3)–C(53)	109.4(6)
N(2)–Ru–Cl(1)	89.3(2)	C(23)–N(3)–Ru	126.7(5)
N(3)–Ru–Cl(1)	87.42(14)	C(53)–N(3)–Ru	123.1(4)
P–Ru–Cl(2)	89.56(6)	N(1)–C(21)–S(1)	111.8(5)
N(1)–Ru–Cl(2)	88.49(14)	C(51)–C(41)–S(1)	105.6(11)
N(2)–Ru–Cl(2)	88.6(2)	C(41)–C(51)–N(1)	119.2(9)
N(3)–Ru–Cl(2)	86.32(14)	N(2)–C(22)–S(2)	114.0(6)
P–Ru–Cl(2)	96.85(6)	C(52)–C(42)–S(2)	106.4(5)
Cl(1)–Ru–Cl(2)	173.37(6)	N(2)–C(52)–C(42)	116.7(6)
C(1C)–P–C(1B)	102.6(3)	N(3)–C(23)–S(3)	116.8(5)
C(1C)–P–C(1A)	100.2(3)	C(53)–C(43)–S(3)	108.7(5)
C(1B)–P–C(1A)	102.2(3)	N(3)–C(53)–C(43)	115.0(6)
C(1C)–P–Ru	117.4(2)	C(2A)–C(1A)–P	120.7(5)
C(1B)–P–Ru	116.5(2)	C(6A)–C(1A)–P	122.7(5)
C(1A)–P–Ru	115.4(2)	C(2B)–C(1B)–P	119.2(5)
C(21)–S(1)–C(41)	93.4(6)	C(6B)–C(1B)–P	122.7(5)
C(42)–S(2)–C(22)	93.9(3)	C(2C)–C(1C)–P	118.3(5)
C(43)–S(3)–C(23)	90.0(4)	C(6C)–C(1C)–P	124.6(5)

contributions have been obtained by following the procedure: (a) the model molecule [$RuCl_2(PH_3)(thz)_3$] was built from the X-ray coordinates of **2** (PH_3 was substituted for PPh_3); (b) the calculations at the B3LYP/LANL2DZ[20] level were performed through the GAUSSIAN 92[20a] package; (c) the charges for the PPh_3 moiety were estimated by starting from the values calculated for [$RuCl_2(NH_3)_3(PH_2Ph)$] at the same level of theory; P(0.230), Cl(−0.110), C_{ortho}(−0.290), C_{meta}(−0.280), C4(−0.320), H_{ortho}(0.335), H_{meta}(0.310), H4(0.320).

Model complexes *trans*,*trans*,*trans*- and *cis*,*trans*,*cis*-[$RuCl_2(PH_3)_2(NH{=}CH_2)_2$] were geometry optimized at the DFT-B3LYP/LANL2DZ level. Corresponding bond distances and angles within the two $NH{=}CH_2$ ligands were restrained to refine to the same value. Other details of the geometry of the $NH{=}CH_2$ ligands are reported in Results (see below).

Results

Structure of [$RuCl_2(PPh_3)(thz)_3$] 2

Bond lengths and angles are listed in Table 2. The complex molecule and the disorder of thz(1) are represented in Fig. 1. It has a pseudo-octahedral arrangement and consists of two chloride anions *trans* each other, one phosphorus atom from PPh_3 and three nitrogen atoms from the thz ligands. The Ru–Cl bond distances [average 2.417(2) Å] are in agreement with the mean value found for other ruthenium(II) compounds (see below, Discussion). The Ru–P distance is 2.299(2) Å, shorter than found for most similar six-co-ordinate complexes of Ru^{II}. The Ru–N bond lengths for **2** are significantly different: 2.082(5) [N(1)], 2.106(5) [N(2)] and 2.183(5) Å [N(3)]. Bond angles in the co-ordination sphere deviate significantly from the idealized values, the largest deviation being found for

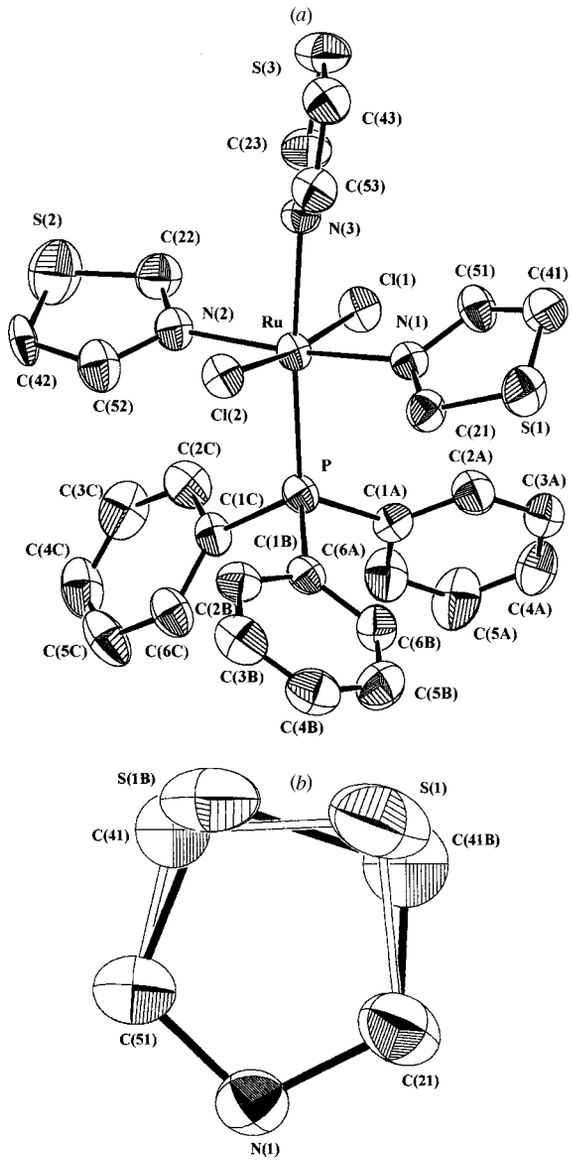

Fig. 1 (*a*) Drawing[21] of the complex molecule [$RuCl_2(PPh_3)(thz)_3$] **2**. Ellipsoids enclose 50% probability. (*b*) Disorder which affects the thz(1) ligand. The two orientations of the ligand moiety around the Ru–N bond axis have occupancies of 0.67 and 0.33

N(1)–Ru–N(2) [173.2(2)°]. The metal centre is almost on the least-squares planes Cl(1)/Cl(2)/N(3)/P [deviation 0.0166(5) Å] and N(1)/N(2)/N(3)/P [0.0241(5)], whereas it deviates significantly [0.1322(6) Å] from the plane Cl(1)/Cl(2)/N(2)/N(1) toward the P donor consistent with a strong Ru–P bond.

The P–C bond lengths average 1.845(6) Å; the Ru–P–C bond angles range from 115.4(2) to 117.4(2)° and the phenyl rings are planar; the phosphorus atom does not deviate significantly from the three planes. The thz(3) and thz(2) systems are not affected by the two-fold type disorder found for thz(1). A discussion of the geometrical parameters for the first two thz moieties is therefore possible. The N–C(2) bond distances [1.276(9) and 1.322(9) Å] are shorter than the N–C(5) ones [1.381(8) and 1.375(9)]. The C–S bond distances have a mean value of 1.683(7). It is worth noting that the Ru–N–C bond angles for the thz(2) ligand are almost equal, whereas for thz(1) and thz(3) the Ru–N–C(2) angles are larger [average 126.4(4)°] than the Ru–N–C(5) ones [average 123.5(4)°]. All the three thz systems are planar, the largest deviation being 0.06(2) Å for C(41). The metal centre deviates 0.0241(5) Å from the least-squares plane N(1)/N(2)/N(3)/P and 0.2013(6), 0.0253(5), and 0.2200(5) Å from the least-squares planes of thz(1), thz(2) and thz(3).

The analysis of the crystal packing did not show any intermolecular stacking interaction involving phenyl rings and thiazole ligands. However, a weak intramolecular stacking interaction is possible between thz(2) and phenyl of PPh_3. The C(1C)···N(2) and C(2C)···C(22) contact distances are 3.34(1) and 3.38(1) Å, respectively, even though the dihedral angle between the two least-squares planes is relatively large, 35.2(2)°. The complex molecules are held together by weak hydrogen bonds of the type C(43)···Cl(2) $(1 - x, -y, -z)$ 3.60(1) Å C(43)–H···Cl(2) 160(2)°.

Physicochemical properties

NMR spectroscopy. Proton NMR data are reported in Table 3, Fig. 2 and SUP 57396. The spectrum of $[RuCl_2(PPh_3)(thz)_3]$ **2** in $CDCl_3$ (see Fig. 2) has signals at δ 9.46 [1 H, H(2), thz *trans* to PPh_3], 9.01 [2 H, H(2), thz *cis* to PPh_3], 8.60 [1 H, H(5), thz *trans* to PPh_3], 8.25 [2 H, H(5), thz *cis* to PPh_3], 7.09 [1 H, H(4), thz *trans* to PPh_3], 7.04 [2 H, H(4), thz *cis* to PPh_3] and 7.4–7.1 (15 H, PPh_3). $CDCl_3$ solutions of **2** are stable for hours at room temperature in the presence of air. The spectrum of $[RuCl_2(PPh_3)_2(thz)_2]$ **1** in $CDCl_3$ shows signals at δ 8.69 [1 H, H(2)], 8.07 [1 H, H(5)] and 6.83 [1 H, H(4)]; therefore the two thz ligands are equivalent. Interestingly the pattern for this solution changes significantly within a few hours while the colour turns from yellow to green, at room temperature under air. We will return to this point below.

The ^1H NMR spectrum of $[Ru(H_2tp)_2(PPh_3)(thz)]Cl_2\cdot 2H_2O$ **3**·$2H_2O$ in $(CD_3)_2SO$ has peaks at δ 8.94 [1 H, H(2) thz], 7.73 [1 H, H(5)] and 7.67 [1 H, H(4)]. The four peaks at δ 8.72, 8.59, 8.52 and 8.27 (1 H each) are attributable to the H(8) and H(2) protons of two H_2tp ligands. This is in agreement with a structure in which PPh_3 and thz are *cis* to each other. The system of peaks at δ 7.34–7.08 is due to the PPh_3 protons. A D_2O solution of **3**·$2H_2O$ showed peaks at δ 8.48, 8.37, 8.16, 8.07, 7.83, 7.51, 7.13 (1 H each) and 6.94 (*ca.* 15 H). Both solutions are stable for hours at room temperature in the air. The compounds

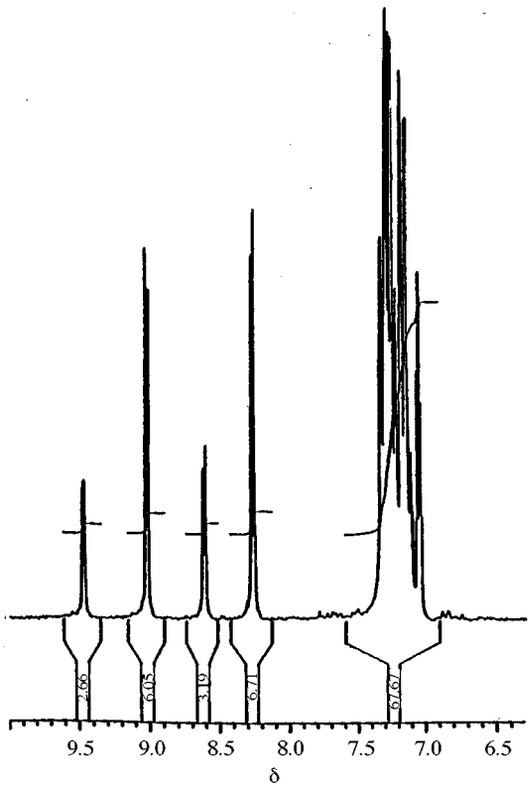

Fig. 2 Proton NMR spectrum of $[RuCl_2(PPh_3)(thz)_3]$ **2** (1×10^{-2} mol dm^{-3}) in $CDCl_3$ at 22 °C

Table 3 Selected ^1H NMR chemical shifts (δ in ppm from $SiMe_4$) for compounds **1**–**5**, **7**, **8** and **10**

In $CDCl_3$					In CD_3OD
1	**2**	thz	**10**	mpym	**8**
	9.46 [H(2) *trans* to PPh_3]		9.26 [H(2)]	9.03 [H(2)]	9.02 [H(8)]
8.69 [H(2)]	9.01 [H(2) *cis* to PPh_3]	8.88 [H(2)]	8.66 [H(6)]	8.52 [H(6)]	8.13 [H(2)]
	8.60 [H(5) *trans* to PPh_3]		6.33 [H(5)]	7.13 [H(5)]	6.90–7.30 ($AsPh_3$)
8.07 [H(5)]	8.25 [H(5) *cis* to PPh_3]	7.98 [H(5)]	2.30 (Me)	2.48 (Me)	
7.40–7.00 (PPh_3)	7.40–7.10 (PPh_3)				
	7.09 [H(4) *trans* to PPh_3]				
6.83 [H(4)]	7.04 [H(4) *cis* to PPh_3]	7.42 [H(4)]			

In $(CD_3)_2SO$					
3	thz	H_2tp	**5**	**4**,**7**	H_2tg
8.94 [H(2) thz]	9.09 [H(2)]		8.76 [H(8)]	8.27 [H(8), **4**]	8.00 [H(8)]
8.72–8.27 [H(2), H(8) H_2tp]		8.34 [H(8)]	8.49 [H(2)]	8.24 [H(8), **7**]	
		8.15 [H(2)]	7.40–7.00 (PPh_3)		
7.73 [H(5) thz]	7.93 [H(5)]		6.10–6.05 [H(1′)]		
7.67 [H(4) thz]	7.74 [H(4)]		5.60–4.90 [H(3′)]		
7.34–7.08 (PPh_3)			5.30–5.20 [H(2′)]		
			4.50–4.10 [H(4′), H(5′)]		

$[Ru(H_2tg)_2(PPh_3)_2]Cl_2\cdot 2H_2O\cdot EtOH$ **4**·$2H_2O$·EtOH and $[Ru(H_2tg)_2(PPh_3)_2][CF_3SO_3]_2\cdot 3H_2O$ **7**·$3H_2O$ show one singlet at δ 8.27 and 8.24 (reference $SiMe_4$) respectively, attributable to the H(8) proton. The signal of **4** is shifted downfield by about 0.27 ppm compared with free H_2tg. The ^1H NMR spectrum of $[Ru(H_2tprta)_2(PPh_3)_2]Cl_2\cdot 3H_2O$ **5**·$3H_2O$ in $(CD_3)_2SO$ has signals at δ 8.76 [H(8)], 8.49 [H(2)], 7.4–7.0 (PPh_3), 6.10–6.05 [H(1′)], 5.6–4.9 [H(3′)], 5.3–5.2 [H(2′)] and 4.1–4.5 [H(4′), H(5′)]. The analysis of the coupling constants and the sugar conformation is discussed below.

The ^1H NMR spectrum of $[Ru^{II}(H_2tp)_2(AsPh_3)(MeOH)]Cl_2\cdot MeOH$ **8**·MeOH in CD_3OD solvent shows two singlets at δ 9.02 and 8.13 with reference to $SiMe_4$ respectively. Multiplets are present in the region between δ 6.90 and 7.30. The two downfield peaks are attributable to the resonances of H(8) and H(2) protons, respectively, of H_2tp. The H(8) : H(2) signal integral ratio is 1.0 : 1, whereas the $AsPh_3$: H(8) ratio is 7.5 : 1. The solid complex **8**, as well as its methanol solutions, are stable for several hours at room temperature also in air. When the ^1H NMR spectrum of **8** was recorded in $(CD_3)_2SO$ solution (at 22 °C) a slow change in the pattern of the downfield peaks occurred. Namely, at least eight peaks clearly appeared in the region attributable to the H(8) and H(2) signals after about 4 h from the mixing. Furthermore, the intensity of the system centered at δ 7.08 (due to the triphenylarsine ligand protons) decreased, while a new absorption centered at δ 7.35 grew in. After 1 week the spectrum showed two singlets at δ 9.67 and 8.71, attributable to the H(8) and H(2) protons of two equivalent H_2tp ligands. The absorption at δ 7.35 had an integral about 7.0 times that of each of the singlets and the signal at δ 7.08 almost disappeared. The NMR pattern in $(CD_3)_2SO$ shows that $AsPh_3$ ligand is easily removed from the $Ru^{II}(H_2tp)_2$ co-ordination sphere, in contrast to the PPh_3 homologues (see below).

The ^1H NMR spectrum of $[RuCl_2(PPh_3)_2(mpym)_2]$ **10** in $CDCl_3$ has peaks at δ 2.30 (3 H, Me), 6.33 [1 H, H(5)], 8.66 [1 H, H(6)] and 9.26 [1 H, H(2)]. This means that the two mpym molecules are equivalent and the *cis*,*cis*,*cis* isomer is excluded. The *trans*,*cis*,*cis* isomer is also excluded on the basis of the magnitude of the shift toward lower field of the signals of H(2) and H(6). The isomers *trans*,*trans*,*trans* and *cis*,*trans*,*cis* are both compatible with the spectrum.

Electrochemistry

The stability of the 6-thiopurine complexes of Ru against oxidation was investigated through electrochemical techniques. The triflate (CF_3SO_3) salts have been prepared to allow an acceptable solubility in acetonitrile, a suitable solvent for these methods. The cyclic voltammetric curve recorded for a 1 mM MeCN (0.1 M $NaClO_4$ as supporting electrolyte) solution of **7** is reported in Fig. 3. By scanning the potential in the anodic direction at a scan rate, ν, of 0.02 V s^{-1} a single catho-anodic system with an anodic peak potential of 1.048 V and a cathodic peak at 0.984 V (*vs.* SCE) was observed. Cyclic voltammetric tests performed at ν ranging from 0.02 to 20 V s^{-1} showed the constancy of the significant quantities $(E_p)_a$, $(E_p)_a - (E_p)_c$, $(i_p)_a/\nu^{\frac{1}{2}}$ and $(i_p)_a/(i_p)_c$. Controlled-potential coulometry carried out at +1.0 V on a solution of **7** (0.1 mmol per 50 cm^3) in MeCN (0.1 M $NaClO_4$) caused the yellow solution to turn brown. After a charge of 1 mol of electrons per mol of **7** had passed the current decreased to 0.4 mA. The mixture was then exhaustively reduced at +0.88 V. The colour turned back to yellow. The final solution was brought to dryness under vacuum with a stream of ultrapure argon.

The solid product was mixed with water at room temperature for 12 h to extract $NaClO_4$. The mixture was then filtered and the insoluble fraction dried under vacuum at room temperature for 3 d. The solid was recrystallized from ethanol. The purified material gave a ^1H NMR spectrum [$(CD_3)_2SO$ solution] superimposable on that of **7**. The yield was about 20%. The relatively low yield of the recovered product can be explained by taking into account at least three factors. First, the concentration of the complex in the starting solution is small (*ca.* 2×10^{-3} M); secondly, the presence of a large amount of supporting electrolyte, 0.1 M $NaClO_4$), increases the loss of the complex during the recovery procedures; thirdly, some decomposition of the ruthenium complexes can occur during the slow coulometric experiment.

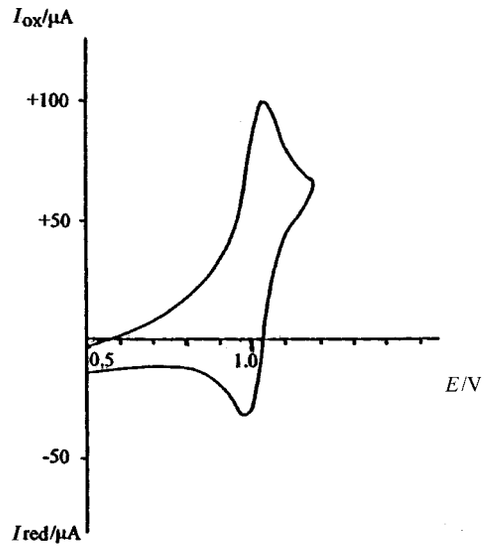

Fig. 3 Cyclic voltammogram of a 1 mM MeCN solution of $[Ru(H_2tg)_2(PPh_3)_2][CF_3SO_3]_2$ (0.1 M $NaClO_4$) at a platinum electrode (*versus* SCE). Scan rate 50 mV s^{-1}

Infrared spectroscopy

The band at 1640 cm^{-1} in the spectrum of $[Ru(H_2tp)_2(PPh_3)(thz)]Cl_2\cdot 2H_2O$ **3**·$2H_2O$ is blue shifted some 35 cm^{-1} with respect to free H_2tp.

Molecular mechanics and density functional analysis

The analysis performed on the molecule $[RuCl_2(PPh_3)(thz)_3]$ **2** reproduced well the solid-state, X-ray diffraction, structure; differences for the geometrical parameters being less than 0.03 Å and 3°, respectively, for the ligand moieties. The computed parameters for the co-ordination sphere are also in good agreement with the experimental values, the largest differences being 0.06 Å ($d_{calc} - d_{exptl}$) for Ru–P and −3.7° ($\theta_{calc} - \theta_{exptl}$) for Cl–Ru–N. The r.m.s. of the deviations of the atoms for the all-atom rigid superimposition of the computed and experimental (X-ray) structures is 0.300 Å, the largest deviations of the atomic positions being found for some of the peripheral H atoms of PPh_3. Analysis of the energy profile against the rotation of thz ligands around the Ru–N bonds showed that two mimima at almost the same energy occur at Cl–Ru–N–C torsion angles of about 120 and 300°. The minimum barrier between the two energy minima averages 8 kcal. Rotation around Ru–N is therefore much hindered at room temperature for thz and the existence of two rotamers is highly probable. Even though the computation has been done for conditions far from the solid state, this molecule mechanics analysis forecasts the existence of C(2) rotamers as regards the thz moiety. This happens in the solid state at least for thz(1).

Starting from the molecular structure of compound **2**, the molecules *trans*,*trans*,*trans*-, *cis*,*trans*,*cis*- and *trans*,*cis*,*cis*-$[RuCl_2(PPh_3)_2(thz)_2]$ (see Scheme 1) have been built *via* MACROMODEL. The three structures have been optimized by using the force field reported in Table 4; the total strain energy was −46.64, −41.17 and −37.10 kcal, respectively. The

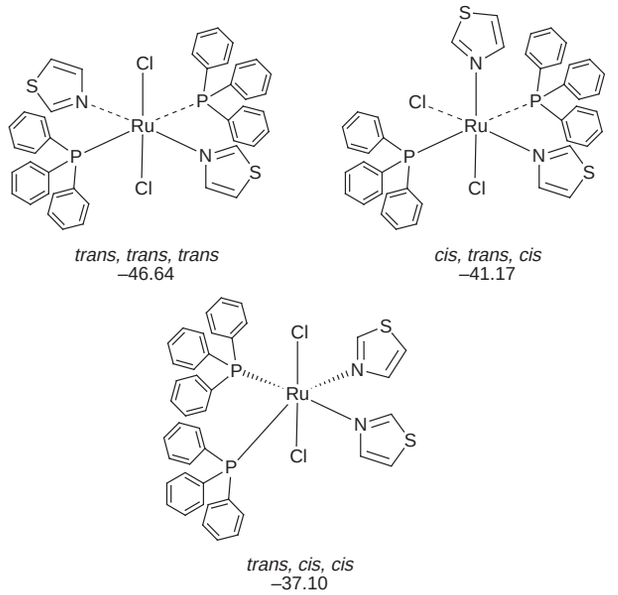

Scheme 1 The isomers of $[RuCl_2(PPh_3)_2(thz)_2]$ which have been investigated *via* molecular mechanics (total strain energy in kcal mol^{-1} of the geometry-optimized structure is shown for each isomer)

Table 4 Force-field parameters used for the simulations of $[RuCl_2(PPh_3)_2(thz)_2]$ **1** and $[RuCl_2(PPh_3)(thz)_3]$ **2**

Vector	R_0/Å	k_r/kcal $Å^{-2}$ mol^{-1}
Ru–N (*trans* N)	2.09	140
Ru–Cl	2.42	90
Ru–P	2.30	250
Ru–N (*trans* P)	2.18	120
P–C	1.84	330
	θ/°	k_θ/kcal rad^{-2} mol^{-1}
Cl–Ru–Cl (*cis*)	90	25
Cl–Ru–Cl (*trans*)	180	10
Cl–Ru–N (*cis*)	90	30
Cl–Ru–N (*trans*)	180	15
Cl–Ru–P	90	25
N–Ru–N (*cis*)	90	35
N–Ru–N (*trans*)	180	20
N–Ru–P (*cis*)	90	30
N–Ru–P (*trans*)	180	15
P–Ru–P (*cis*)	90	30
P–Ru–P (*trans*)	180	15
Ru–P–C	109	25

steric hindrance between the PPh_3 ligands (shown by the computed bond angles P–Ru–P 104.2 and N–Ru–N 78.4°) for *trans*,*cis*,*cis*-$[RuCl_2(PPh_3)_2(thz)_2]$ is mostly responsible for the difference.

As suggested by one of the referees, DFT calculations and geometry optimizations at the Becke3LYP/LANL2DZ level (see Experimental section) have been performed for the *trans*,*trans*,*trans*- and *cis*,*trans*,*cis*-$[RuCl_2(PH_3)_2(NH{=}CH_2)_2]$ isomers as models for $[RuCl_2(PPh_3)_2(thz)_2]$. The optimized structure for the *trans*,*trans*,*trans* isomer has Ru–Cl, Ru–P and Ru–N bond distances of 2.510, 2.421 and 2.056 Å respectively. The two $NH{=}CH_2$ ligands have a head-tail arrangement. It is evident that the computed Ru–Cl distance is significantly longer (*ca.* 0.1 Å) than the experimental values (solid state) found in this work as well as in other ruthenium(II) compounds (see above). On the contrary, the experimental Ru–P and Ru–N bond distances are well reproduced by theory. The computed metal–donor distances for the *cis*,*trans*,*cis* isomer are Ru–Cl 2.518, Ru–P 2.416 and Ru–N 2.050 Å. The total energy for the optimized *trans*, *trans*,*trans* and *cis*,*trans*,*cis* isomers differs by 4.04 kcal mol^{-1}, *trans*,*trans*,*trans* being the most stable. Noteworthy, the P–Ru–P angle for *cis*,*trans*,*cis* is 163.4° whereas for *trans*,*trans*,*trans* it is 179.6°.

Discussion

Structure of $[RuCl_2(PPh_3)(thz)_3]$

Comparison of the co-ordination-sphere geometry of $[RuCl_2(PPh_3)(thz)_3]$ **2** and related complexes found in the literature shows a perfect agreement for Ru–Cl bond distances; see, for examples, $[RuCl_2(PPh_3)_3]$ [2.387(7)],[22] *trans*,*cis*,*cis*-$[RuCl_2(dmso)_2(NH_3)_2]$ [2.4077(7)][23] and $[RuCl_2(pnp)(PPh_3)]$ [pnp = 2,6-bis(diphenylphosphinomethyl)pyridine, 2.4192(7) Å].[24]

The Ru–P bond length for complex **2** compares well with the distances found for [RuCl(D,L-histidinate)$(PPh_3)_2$] [2.277(2) and 2.338(2)][25] and for $[Ru(NC_5H_4S)_2(CO)(PPh_3)]$[26a] [2.309(1) Å]. For five-co-ordinate $[RuCl_2(PPh_3)_3]$ the Ru–P vectors *trans* to each other measure 2.374(6) and 2.412(6) Å, whereas the third phosphorus is 2.230(8) from the metal.[22] The Ru–P bond distances relevant to the two vectors *trans* to each other for $[RuCl_2(pnp)(PPh_3)]$ are 2.3682(7) and 2.3641(7) Å, whereas the Ru–P bond *trans* to N measures 2.3401(7) Å.[24] Other Ru–P bond lengths range from 2.339(2) to 2.399(6).[26] Longer Ru–P distances [2.453(3) and 2.522(3) Å] have been found for *trans*,*trans*,*trans*-$[Ru(quin)_2(PPh_3)_2]$ (Hquin = 8-hydroxyquinoline).[27] On a balance, the Ru–P bond distance found for **2** is somewhat shorter than analogous lengths. This suggests a relatively high thermodynamic stability of the Ru–P bond of **2**. We reasoned that substitution reactions on **2** with thiopurines can remove chloride (usually behaving as a good leaving donor) and thz ligands first, to produce cationic complex molecules. In fact the reaction of **2** and H_2tp produced $[Ru(H_2tp)_2(PPh_3)(thz)]Cl_2$ **3** by removing two chloride anions and two thz molecules from the co-ordination sphere.

The long Ru–N bond distance *trans* to P is in agreement with the length of 2.168(2) Å found for N *trans* to P in $[RuCl_2(pnp)(PPh_3)]$[24] and of 2.15(1) and 2.16(1) Å for $[Ru(H_2tp)_2(PPh_3)_2]^{2+}$.[4b] Agreement is noted also with the Ru–N bond distances [2.202(6) and 2.160(6) Å] of $[RuCl_3(metet)(PPh_3)]$ (metet = methionine ethyl ester).[25] For $[RuCl(H)(CO)(PPh_3)_2(SN_2C_6H_4)]$[26d] ($SN_2C_6H_4$ = 2,1,3-benzothiadiazole) and $[Ru(Htddt)_2(CO)(PPh_3)_2]$[26b] (tddt = 1,3,4-thiadiazole-2,5-dithiolate) the Ru–N vectors *trans* to CO measure 2.177(5) and 2.18(1) Å, respectively, showing that the *trans* influences of PPh_3 and CO must be similar in this type of six-co-ordinated ruthenium(II) complexes. The Ru–N(1) and Ru–N(2) bond lengths for **2** are in agreement with the value of 2.087(1) Å for the Ru–N (imidazole) distance[28] and the mean value of 2.068(9) Å found for *trans*,*trans*,*trans*-$[RuL_2(PPh_3)_2]$.[27]

The bond distances of the thz ligands are in agreement with a higher character of double bond for N–C(2) compared with N–C(5), whereas the C(4)–C(5) bond distances [average 1.406(8) Å] are longer than a pure C=C double bond.

Finally it should be noted that the analysis of the structures of metal–thiazole complexes carried out in this laboratory (present work and ref. 5) reveals that the thiazole ligand is often affected by a two-fold disorder around the MN bond. This type of disorder is easily detected with a ligand such as thiazole because S and CH have significantly different electron densities. We think that the same type of disorder can occur for metal–imidazole groups even at a higher frequency than for metal–thiazole. On the contrary, reports of disorder for metal–imidazole groups are uncommon to our knowledge. This must be due to the strict similarity of the electron densities of NH and CH groups as well as of C=C and C–N bond lengths.

Physicochemical properties

NMR spectroscopy. The chemical shifts of H(2) and H(5) of the thz ligands of $[RuCl_2(PPh_3)(thz)_3]$ **2** are moved toward lower

$$[RuCl_2(PPh_3)_2(thz)_2] \rightleftharpoons [RuCl_2(PPh_3)(thz)_2] + PPh_3 \quad (1)$$

$$[RuCl_2(PPh_3)(thz)_2] + thz \rightleftharpoons [RuCl_2(PPh_3)(thz)_3] \quad (2)$$

$$6[RuCl_2(PPh_3)_2(thz)_2] \rightleftharpoons 4[RuCl_2(PPh_3)(thz)_3] + [\{RuCl_2(PPh_3)_2\}_2] + 4\ PPh_3 \quad (3)$$

Scheme 2 Equilibria which occur in solutions of complex **2** (5×10^{-2} M) in $CDCl_3$ at room temperature

field {free thz gives signals at δ 8.88 [H(2)], 7.98 [H(5)] and 7.42 [H(4)][29] whereas that of H(4) is moved upfield, upon co-ordination. It should be noted that the ^{1}H NMR spectra of *trans*-$[PtCl_2(thz)_2]$,[30] $[RhCl_2(Ph)(SbPh_3)(thz)_2]$[5] and $[RhCl_2(Ph)(SbPh_3)_2(thz)]$[5] have all the signals of the thz protons deshielded with respect to those of free thz. The high *trans* influence of PPh_3 related to its π-accepting behaviour is in agreement with the high deshielding effect experienced by the thz(3) protons. Finally the effect on the chemical shifts of H(2) and H(5) is consistent with metal co-ordination to N instead of S, also in solution.

The equivalence of the two thz ligands of $[RuCl_2(PPh_3)_2(thz)_2]$ **1** is in accord with *trans*,*trans*,*trans*, *trans*,*cis*,*cis* or *cis*,*trans*,*cis* co-ordination. Larger downfield shifts are expected for *trans*,*cis*,*cis* so this isomer can be ruled out. The molecular mechanics and molecular orbital analysis reported above shows that the *trans*,*trans*,*trans* isomer is the most stable. It is assumed that this is the species in the solid state and in chloroform solution. The signals of H(2) and H(4) are shielded with respect to free thz, whereas that of H(5) is slightly deshielded. The signals of the PPh_3 protons are in the range δ 7.0–7.4.

A small signal centered at δ 7.33 appears in the spectra of solutions prepared some 10 min before recording the spectra. This is attributable to free PPh_3 and means that complex **1** slowly releases PPh_3 in chloroform. To investigate the evolution of the system several spectra were recorded at increasing times. After about 3 h (at 25 °C) signals attributable to protons of **2** are evident. After 24 h from mixing of **1** and $CDCl_3$ the solution is deep green and signals attributable to **1**, **2** and free PPh_3 are all present. Both **1** and **2** gave a yellow solution immediately after mixing with $CDCl_3$. As no other signals attributable to free or bound thz protons are present in the spectrum of the green solution, the compounds responsible for this colour contain just Cl^- and PPh_3 as ligands. It is possible that the green colour comes from $[RuCl_2(PPh_3)_2]_2$[31] which also forms from $[RuCl_2(PPh_3)_3]$ in $CDCl_3$. Other products are $[RuCl_2(PPh_3)(thz)_3]$ **2** (yellow) and PPh_3. Peaks found in the spectrum of a green solution obtained from $[RuCl_2(PPh_3)_3]$ are present also in the spectrum of the green solution obtained from **1**. The process of decomposition of **1** should start with the dissociation of PPh_3 [Scheme 2, equation (1)]; this is reasonable owing to the high *trans* influence of PPh_3 itself in the *trans*,*trans*,*trans* isomer. The addition of an excess of PPh_3 to the solution stops the formation of the green species. On the other hand the addition of thz prevents the formation of the green species but favours the formation of $[RuCl_2(PPh_3)(thz)_3]$ [Scheme 2, equation (2)]. After some 24 h from the dissolution of **1** in $CDCl_3$ an equilibrium is reached and the molar ratio $[RuCl_2(PPh_3)_2(thz)_2]$:$[RuCl_2(PPh_3)(thz)_3]$ is *ca.* 1.7:1 (as measured from the peak integrals), when the initial concentration of **1** is 5×10^{-2} M (without any excess of PPh_3 or thz). The full process is represented in Scheme 2, equation (3).

The presence of air (oxygen) catalyses the reaction. Under an atmosphere of pure nitrogen, solutions of complex **1** in $CHCl_3$ do not show any green colour even after 72 h. The same solution under an atmosphere of pure oxygen becomes dark green (after *ca.* 0.3 h) faster than when air is bubbled into the solution. Molecular oxygen can bring about ruthenium(III) species making the overall processes (Scheme 2) faster. Oxygen can also oxidise PPh_3 to $OPPh_3$, so increasing the yield of the green compound.

The peak pattern for $[Ru^{II}(H_2tp)_2(PPh_3)(thz)]^{2+}$ is consistent with *cis* chelating [S(6)/N(7)] H_2tp molecules, and PPh_3 and thz ligands also *cis* to each other; this suggests that the thz molecule *trans* to P of $[RuCl_2(PPh_3)(thz)_3]$ is removed first, then the two chloride donors and a further thz molecule escape the co-ordination sphere. On the basis of the geometries previously found for other Ru^{II}–H_2tp/Htpr (Htpr = purine-6-thione-9-riboside) derivatives[4] one expects that the two S(6) donors of $[Ru^{II}(H_2tp)_2(PPh_3)(thz)]^{2+}$ are *trans* each other. The infrared data are consistent with metal co-ordination to S(6) and proton retention on N(1).[5,32] The absence of any detectable band in the range 1090–1230 cm^{-1} as opposed to the presence of an absorption at 1150 cm^{-1} in the spectrum of free 6-thiopurine, attributed to the C=S stretching vibration, is in accord with the metal co-ordination of S.[33–36]

The ^{1}H NMR data for $[Ru(H_2tg)_2(PPh_3)_2]Cl_2$ and $[Ru(H_2tg)_2(PPh_3)_2][CF_3SO_3]_2$ are in agreement with a structure for $[Ru(H_2tg)_2(PPh_3)_2]^{2+}$ similar to that found for $[Ru(H_2tp)_2(PPh_3)_2]^{2+}$[4b] and $[Ru(Htpr)_2(PPh_3)_2]^{2+}$.[4a] It should be noted that the X-ray diffraction powder patterns recorded for the H_2tp and H_2tg derivatives (counter ion Cl^-) are very similar to each other.

The analysis of the electrochemical data shows that $[Ru(H_2tg)_2(PPh_3)_2]^{2+}$ undergoes oxidation to ruthenium(III) species [at *ca.* 1.0 V (SCE) in acetonitrile]. It is reasonable to assume the formation of $[Ru(H_2tg)_2(PPh_3)_2]^{3+}$ which is reduced back to $[Ru(H_2tg)_2(PPh_3)_2]^{2+}$ when the potential is decreased to 0.88 V. The parameters reported above (Results) indicate a quasi-reversible monoelectronic charge transfer without any coupled chemical reaction on the timescale for this technique and the calculated $E_{\frac{1}{2}}$ value is 1.02 V (SCE) or 0.590 V (ferrocene–ferrocenium). A reasonable event is the retention of the co-ordination sphere. The relatively high value for $E_{\frac{1}{2}}$ explains the stability of the complexes to oxidation by air. The presence of chelate ligands makes the d^6 strong field co-ordination sphere highly kinetically inert towards substitution. The inertness of the d^5 ruthenium(III) species formed by electrochemical oxidation should be lower and some decomposition of the oxidized species is more probable, during the slow coulometric experiment. Finally, it should be recalled that $[Ru(bipy)_3]^{2+}$ exhibits $E_{\frac{1}{2}} = 0.89$ V[37] (ferrocene–ferrocinium) in acetonitrile which means that the oxidation of $[Ru(H_2tg)_2(PPh_3)_2]^{2+}$ is somewhat easier than that of the tris(bipyridine) derivative.

The ^{1}H NMR signals for $[Ru(H_2tprta)_2(PPh_3)_2]^{2+}$ are consistent with one C(2) diastereoisomer roughly twice as abundant as the other. The ^3J(H1′H2′) values (3.0 and 2.5 Hz) for the diastereoisomers with H(1′) signals at δ 6.10 and 6.05 suggest that the ribose prefers the C(2′)-*endo* conformation.[38] The ^{31}P NMR spectrum has two signals (δ 42.54 and 41.86, trimethylphosphate). The spectrum of free PPh_3 has a signal at δ −9.2.

The experiments carried out in this work on the triphenylarsine derivatives show that the reaction of the green crystalline powder $[Ru^{III}Cl_3(AsPh_3)_2(MeOH)]$ with H_2tp, in a 1:2 molar ratio, produces the crystalline orange compound $[Ru^{II}(H_2tp)_2(AsPh_3)(MeOH)]Cl_2$·MeOH **8**·MeOH. The reduction of the metal centre occurs in the presence of air as well as under ultrapure argon. The mixture of $[Ru^{III}Cl_3(AsPh_3)_2(MeOH)]$ in Me_2SO turns brown and then orange under ultrapure argon when heated at 60 °C for 20 min. The orange solution produces crystals of $[Ru^{II}Cl_2(Me_2SO)_4]$. The ^{1}H NMR data for **8** show the equivalence of the two H_2tp ligands and that $AsPh_3$ and MeOH ligands are *trans* to each other. These effects can be interpreted on the basis of a nucleophilic substitution of $AsPh_3$ and MeOH by Me_2SO. Whereas almost complete substitution occurs within 5 h at 40 °C, the H_2tp molecules are not removed under these conditions.

Molecular mechanics and density functional analysis

Even though the molecular mechanics technique is not very appropriate for discriminating among different isomers because electronic effects are not taken into account, the differences in the total strain energy of the isomers *trans*,*trans*,*trans*-, *cis*,*trans*,*cis*- and *trans*,*cis*,*cis*-$[RuCl_2(PPh_3)_2(thz)_2]$ are larger than 4 kcal mol^{-1} and the trend is reasonable. We recall that electrostatic and solvation effects (chloroform as solvent) have been taken into account. Therefore, for $[RuCl_2(PPh_3)_2(thz)_2]$, the isomer with the smallest total strain energy, namely *trans*, *trans*,*trans*, can be considered the most probable. The analysis of molecular orbital calculations carried out on the *trans*,*trans*, *trans* and *cis*,*trans*,*cis* isomers confirms the finding of molecular mechanics. It is interesting that the difference in the total strain energies (5.47 kcal) is higher than that in the total energies computed *via* DFT methods for the $[RuCl_2(PH_3)_2(NH{=}CH_2)_2]$ model (4.04 kcal).

Conclusion

This work has provided information on the following.

(a) The reactivity of 1,3-thiazole with Ru^{II}, at least in the case of $[RuCl_2(PPh_3)_3]$ as the starting compound. The complex $[RuCl_2(PPh_3)(thz)_3]$ can be isolated in high yield when two phosphine ligands per ruthenium centre are removed in two steps; thz always binds to the metal by nitrogen and not by sulfur. This seems to be a common behaviour even towards other platinum-group metals.[5,29] A 1:10 excess of thz at the temperature of refluxing ethanol is not enough to remove the last phosphine ligand from $[RuCl_2(PPh_3)(thz)_3]$. This goal is also not reached by reaction of $[RuCl_2(PPh_3)(thz)_3]$ with H_2tp in ethanol, which allows removal of thz molecules and the two chloride ions but not of the PPh_3 ligand.

(b) The reactivity of H_2tp with Ru^{II}. It is confirmed, that as reported by us previously, H_2tp and some of its analogues behave as chelating agents *via* S(6)/N(7). Species of the type $[Ru(H_2tp)_2(PPh_3)_2]Cl_2$ are less water soluble than $[Ru(H_2tp)_2(PPh_3)(thz)]Cl_2$ probably because of the presence of two highly hydrophobic PPh_3 systems instead of one. The complex $[Ru^{II}(H_2tg)_2(PPh_3)_2]^{2+}$ can be electrochemically oxidized to $[Ru^{III}(H_2tg)_2(PPh_3)_2]^{3+}$ in acetonitrile without any gross change of the co-ordination sphere. The synthesis of water-soluble ruthenium–thiopurine complexes is interesting for performing experiments with biological molecules or for cytostatic tests.

(c) The reactivity of $[Ru^{III}Cl_3(AsPh_3)_2(MeOH)]$ with H_2tp in methanol. The addition of H_2tp to a suspension of $[Ru^{III}Cl_3(AsPh_3)_2(MeOH)]$ in refluxing methanol results in a decrease in the oxidation number from Ru^{III} to Ru^{II} and the formation of $[Ru^{II}(H_2tp)_2(AsPh_3)(MeOH)]^{2+}$.

Acknowledgements

R. C. thanks Professor A. Cinquantini, Università di Siena, for the electrochemical measurements. Financial support from Università di Siena, fund 60%, and from Consiglio Nazionale delle Ricerche (CNR), Roma, is acknowledged. Mr. Francesco Berrettini, Centro Interdipartimentale di Analisi e Determinazioni Strutturali, Università di Siena, is acknowledged for X-ray data collection.

References

1 (*a*) J. Reedijk, *J. Chem. Soc.*, *Dalton Trans.*, 1996, 801; (*b*) Y. Chen, F.-T. Lin and R. E. Shepherd, *Inorg. Chem.*, 1997, **36**, 818; (*c*) M. Hartmann, T. J. Einhäuser and B. K. Keppler, *Chem. Commun.*, 1996, 1741; (*d*) L. M. Torres and L. G. Marzilli, *J. Am. Chem. Soc.*, 1991, **113**, 4678; (*e*) S. Mukundan, jun., Y. Xu, G. Zon and L. G. Marzilli, *J. Am. Chem. Soc.*, 1991, **113**, 3021; (*f*) M. Krumm, I. Mutikainen and B. Lippert, *Inorg. Chem.*, 1991, **30**, 890; (*g*) L. G. Marzilli, *New J. Chem.*, 1990, **14**, 409 and refs. therein; (*h*) E. L. M. Lempers and J. Reedijk, *Inorg. Chem.*, 1990, **29**, 1880; (*i*) M. J. Bloemink, E. L. M. Lempers and J. Reedijk, *Inorg. Chim. Acta*, 1990, **76**, 317; (*j*) S. E. Sherman and S. Lippard, *Chem. Rev.*, 1987, **87**, 1153 and refs. therein; (*k*) P. Köpf-Maier and H. Köpf, *Chem. Rev.*, 1987, **87**, 1137 and refs. therein; (*l*) B. Lippert, *Prog. Inorg. Chem.*, 1989, **37**, 1 and refs. therein; (*m*) E. Alessio, Y. Xu, S. Cauci, G. Mestroni, F. Quadrifoglio, P. Viglino and L. G. Marzilli, *J. Am. Chem. Soc.*, 1989, **111**, 7068; (*n*) H. R. Rubin, T. P. Haromy and M. Sundaralingam, *Acta Crystallogr.*, *Sect. C*, 1991, **47**, 1712; (*o*) K. Aoki, M. Moshino, T. Okada, H. Yamazaki and H. Sekizawa, *J. Chem. Soc.*, *Chem. Commun.*, 1986, 314; (*p*) D. W. Abbott and C. Woods, *Inorg. Chem.*, 1983, **22**, 597; (*q*) R. J. Broomfield, R. H. Dainty, R. D. Gillard and B. J. Heaton, *Nature* (*London*), 1969, **223**, 735; (*r*) B. Rosenberg, in *Metal Ions in Biology*, ed. T. G. Spiro, Wiley, New York, 1980, vol. 1, ch. 1.

2 (*a*) C. J. Zubrod, *Life Sci.*, 1974, **14**, 809; (*b*) D. R. Williams, *Chem. Rev.*, 1972, **72**, 203; (*c*) H. B. Wood, jun., *Cancer Chemother. Rep.*, Part 3, 1971, **2**, 9; (*d*) *Comprehensive Medicinal Chemistry*, eds. C. Hansch, P. G. Sammes, J. B. Taylor, J. C. Emmett, P. D. Kennewell and C. A. Ramsden, Pergamon, Oxford, 1990.

3 C. M. Dupureur and J. K. Barton, *Inorg. Chem.*, 1997, **36**, 33; M. R. Arkin, E. D. A. Stemp, R. E. Holmlin, J. K. Barton, A. Hormann, E. J. C. Olson and P. F. Barbara, *Science*, 1996, **273**, 475; A. M. Pyle and J. K. Barton, *Prog. Inorg. Chem.*, *Bioinorg. Chem.*, 1990, **38**, 413.

4 (*a*) R. Cini, R. Bozzi, A. Karaulov, M. B. Hursthouse, A. Calafat and L. G. Marzilli, *J. Chem. Soc.*, *Chem. Commun.*, 1993, 899; (*b*) R. Cini, A. Cinquantini, M. Sabat and L. G. Marzilli, *Inorg. Chem.*, 1985, **24**, 3903.

5 A. Cavaglioni and R. Cini, *J. Chem. Soc.*, *Dalton Trans.*, 1997, 1149; *Polyhedron*, 1997, **16**, 4045.

6 P. J. Brothers, *Prog. Inorg. Chem.*, 1981, **28**, 1; D. E. Fogg, B. R. James and M. Kilner, *Inorg. Chim. Acta*, 1994, **222**, 85.

7 A. Cinquantini, R. Cini, R. Seeber and P. Zanello, *J. Electroanal. Chem.*, 1980, **111**, 309.

8 T. A. Stephenson and G. Wilkinson, *J. Inorg. Nucl. Chem.*, 1966, **28**, 945.

9 G. M. Sheldrick, SHELXS 86, Program for Crystal Structure Determination, University of Göttingen, 1986.

10 G. M. Sheldrick, SHELXL 93, Program for Crystal Structure Refinement, University of Göttingen, 1993.

11 M. Nardelli, PARST 95, A System of Computer Routines for Calculating Molecular Parameters from Results of Crystal Structure Analysis, University of Parma, 1995.

12 F. Mohamadi, N. G. J. Richars, W. C. Guida, R. Liskamp, M. Lipton, C. Caufield, G. Chang, T. Hendrickson and W. C. Still, *J. Comput. Chem.*, 1990, **11**, 440.

13 W. D. Cornell, P. Cieplak, C. I. Bayly, I. R. Gould, K. M. jun. Merz, D. M. Ferguson, D. C. Spellmeyer, T. Fox, J. W. Caldwell and P. A. Kollman, *J. Am. Chem. Soc.*, 1995, **117**, 5179.

14 R. M. Badger, *J. Chem. Phys.*, 1934, **2**, 128.

15 R. M. Badger, *J. Chem. Phys.*, 1935, **3**, 710.

16 D. R. Hershbach and V. W. Laurie, *J. Chem. Phys.*, 1961, **35**, 458.

17 A. Halgren, *J. Mol. Struct.* (*THEOCHEM*), 1988, **163**, 431.

18 A. Halgren, *J. Am. Chem. Soc.*, 1990, **112**, 4710.

19 S. Geremia and M. Calligaris, *J. Chem. Soc.*, *Dalton Trans.*, 1997, 1541.

20 (*a*) GAUSSIAN 92/DFT, Revision F.2, M. J. Frisch, G. W. Trucks, H. B. Schlegel, P. M. W. Gill, B. G. Johnson, M. W. Wong, J. B. Foresman, M. A. Robb, M. Head-Gordon, E. S. Reploge, R. Gomperts, J. L. Andres, K. Raghavachari, J. S. Binkley, C. Gonzales, R. L. Martin, D. J. Fox, D. J. Defrees, J. Baker, J. J. P. Stewart and J. A. Pople, Gaussian, Inc., Pittsburgh PA, 1993; (*b*) A. D. Becke, *J. Chem. Phys.*, 1988, **88**, 1053; (*c*) C. Lee, W. Yang and R. G. Parr, *Phys. Rev. B*, 1988, **37**, 785.

21 L. Zsolani, XPMA and ZORTEP, Interactive ORTEP Programs, University of Heidelberg, 1994.

22 S. J. La Placa and J. A. Ibers, *Inorg. Chem.*, 1965, **4**, 778.

23 M. Henn, E. Alessio, G. Mestroni, M. Calligaris and W. M. Attia, *Inorg. Chim. Acta*, 1991, **187**, 39.

24 L. Barloy, S. Y. Ku, J. A. Osborn, A. De Cian and J. Fischer, *Polyhedron*, 1996, **16**, 291.

25 W. S. Sheldrick and R. Exner, *Inorg. Chim. Acta*, 1992, **195**, 1.

26 (*a*) P. Mura, B. G. Olby and S. D. Robinson, *J. Chem. Soc.*, *Dalton Trans.*, 1985, 2101; (*b*) P. Mura, B. G. Olby and S. D. Robinson, *Inorg. Chim. Acta*, 1985, **97**, 45; (*c*) M. F. McGuiggan and L. H. Pignolet, *Inorg. Chem.*, 1982, **21**, 2523; (*d*) N. W. Alcock, A. F. Hill and M. S. Roe, *J. Chem. Soc.*, *Dalton Trans.*, 1990, 1737.

27 M. Menon, A. Pramanik, N. Bag and A. Chakravorty, *J. Chem. Soc.*, *Dalton Trans.*, 1995, 1417.

28 A. G. Orpen, L. Brammer, F. H. Allen, O. Kennard, D. G. Watson and R. Taylor, *J. Chem. Soc.*, *Dalton Trans.*, 1989, S1.
29 M. M. Muir, M. E. Cadiz and A. Balz, *Inorg. Chim. Acta*, 1988, **151**, 209.
30 M. Van Beusichem and N. Farrell, *Inorg. Chem.*, 1992, **31**, 634.
31 (*a*) P. W. Armit, A. S. F. Boyd and T. A. Stephenson, *J. Chem. Soc.*, *Dalton Trans.*, 1975, 1663; (*b*) P. R. Hoffman and K. G. Caulton, *J. Am. Chem. Soc.*, 1975, **97**, 4221.
32 N. Kottmair and W. Beck, *Inorg. Chim. Acta*, 1979, **34**, 137.
33 L. J. Bellamy, *The Infrared Spectra of Complex Molecules*, Chapman and Hall, London, 1975, vol. 1.
34 A. Grigoratou and N. Katsaros, *Inorg. Chim. Acta*, 1985, **108**, 41.
35 R. Barbieri, E. Rivarola and F. Di Bianca, *Inorg. Chim. Acta*, 1985, **25**, 131.
36 N. Katsaros and A. Grigoratou, *J. Inorg. Biochem.*, 1985, **25**, 131.
37 M. Gleria, F. Minto, G. Beggiato and P. Bortolus, *J. Chem. Soc.*, *Chem. Commun.*, 1978, 285.
38 G. Altona and M. Sundaralingam, *J. Am. Chem. Soc.*, 1973, **95**, 2333.

Received 19*th March* 1998; *Paper* 8/02175I